Surface nanopatterning through styrene adsorption on Si(100)

A. Calzolari*
INFM-CNR-S3, National Research Center on NanoStructures and BioSystems at Surfaces, I-41100 Modena, Italy

A. Ruini and E. Molinari
INFM-CNR-S3, National Research Center on NanoStructures and BioSystems at Surfaces, I-41100 Modena, Italy and Dipartimento di Fisica, Universitá di Modena e Reggio E., I-41100 Modena, Italy

M. J. Caldas
Istituto de Fisica, Universidade de Sao Paulo, 05508-900 Sao Paulo, Brazil and INFM-CNR-S3, National Research Center on NanoStructures and BioSystems at Surfaces, I-41100 Modena, Italy
(Received 13 September 2005; published 22 March 2006)

We present an *ab initio* study of the electronic properties of styrene molecules adsorbed on the dimerized Si(100) surface, ranging from the single molecule to the full monolayer (ML). The adsorption mechanism primarily involves the vinyl group via a [2+2] cycloaddition process that leads to the formation of covalent Si—C bonds and a local surface derelaxation, while it leaves the phenyl group almost unperturbed. The investigation of the functionalized surface as a function of the coverage (e.g., 0.5–1 ML) and of the substrate reconstruction reveals two major effects. The first results from Si dimer-vinyl interaction and concerns the controlled variation of the energy band gap of the interface. The second is associated to phenyl-phenyl interactions, which give rise to a regular pattern of electronic wires at surface, stemming from the π-π coupling. These findings suggest a rationale for tailoring the nanopatterning of the surface in a controlled way.

DOI: 10.1103/PhysRevB.73.125420 PACS number(s): 68.43.Bc, 82.40.Np, 73.20.At, 71.15.Mb

I. INTRODUCTION

Nanopatterning of surfaces through organic molecules[1] represents a viable route to handle the properties of conventional materials, in view of their future technological (nanoelectronics, nonlinear optics, optoelectronics, etc.) and bioengineering applications (sensor activity, molecular recognition, etc.).[2] In particular, the functionalization of semiconductor surfaces[3] allows one to obtain nanostructured materials, whose properties may be tuned in controlled ways. While molecular bonding on metals (e.g., thiol/Au) is typically non-site-specific,[4] the localized and directional character of semiconductor bonds at surfaces is able to impart an ordered arrangement to the adsorbed molecules, making the substrate an intrinsic template for the growth of the molecular layer.

The reconstructed (100) silicon surface seems particularly suited to couple to the carbon atoms of the organic molecules.[3] Since the surface reactivity is essentially ruled by the presence of dangling bonds at the surface, most experiments were done using the hydrogen terminated Si substrates, in order to prevent spurious oxidation processes.[5–7] On the other hand, the clean Si(100) surface exhibits a Si═Si dimerlike motif, whose electronic properties are in close analogy to those of the carbon-carbon double bond (C═C) of alkenes. Recent experiments have demonstrated that unsaturated hydrocarbons (e.g., ethylene,[8,9] benzene,[10] cyclopentene,[11,12] etc.) may easily react with Si═Si dimers, forming stable organic/semiconductor interfaces. Moreover, the direct measurement of the transport properties through single molecules (e.g., styrene, cyclopentene, TEMPO[12,13]) on dimerized Si(100) has recently shown the possibility of realizing operational semiconductor-based molecular devices.[14,15]

Despite the increasing interest in organic adsorption on the Si(100) surface, only very recently more detailed theoretical studies been reported;[16–25] most of the existing works dealt with the adsorption geometries or the reaction pathways, and, in particular for styrene,[16,17] the activated absorption on the monohydride (2×1) surface was studied both by cluster and extended surface methods, but did not focus on the electronic properties, while absorption on the clean surface was only studied through a cluster model,[25] which cannot gauge the effects on the surface electronic states.

In this paper, we present a first-principles investigation of the electronic properties of styrene adsorbed on the clean Si(100) surface. This system is a representative model for hybrid organic/surface interfaces,[13,26,27] since styrene is constituted of two building blocks [Fig. 1(a)], i.e., the phenyl (—C_6H_5) and the vinyl (—CH—CH_2) group, that are the key-components of most conjugated molecular structures and organic polymers. By means of a periodic solid-state approach, we studied the structural and electronic properties of the styrene/Si interface in the case of isolated molecule absorption, as well as full- and half-monolayer coverage. Our results indicate that the properties of the nanopatterned surface can be selectively engineered by tuning the dosage conditions for the adsorption.

II. METHODOLOGY

Our goal is to study a hybrid organic-semiconductor system, at different regimes of organization: the limit of isolated molecule absorbed on the clean surface, and dense absorbed monolayers of the conjugated molecules. Density functional theory (DFT) approaches describe well the bonding proper-

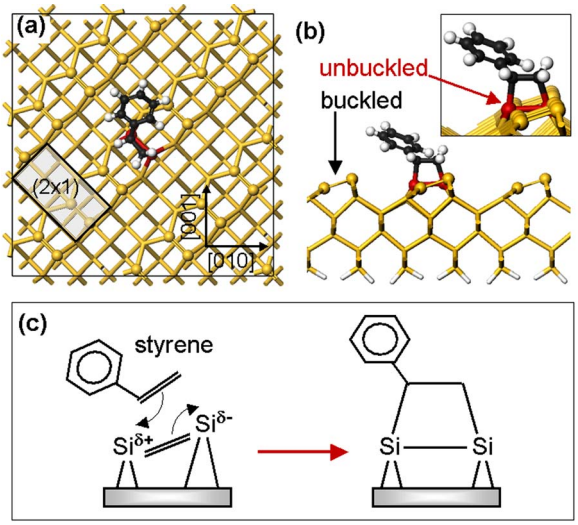

FIG. 1. (Color online) Top (a) and side view (b) of a single styrene molecule adsorbed on a Si(110)-(2×1) surface, simulated in a $c(16\times16)$ cell [shaded area defines the primitive $p(2\times1)$ cell]. Balls identify the atoms of the first layer. Si-dimer rows are aligned along the [011] direction; adsorption site is highlighted in red. The inset zooms into the locally unbuckled adsorption site. (c) Schematic illustration of [2+2] cycloaddition of styrene on the Si(100)-2×1 surface. The reaction, formally forbidden by symmetry constraints, is instead facilitated by the asymmetry of the surface reconstruction, with the consequent charge transfer (δ) between Si atoms.

ties at the interface, giving an accurate description of the bonding lengths and angles for the isolated-molecule limit; however, DFT completely neglects the so-called nonbonding interactions (such as Van der Waals, dispersion, and London forces).[28] On the other hand, nonbonded interactions rule the structural arrangement of supramolecular π-aggregates,[29] and, therefore, any kind of approach that does not include such interactions cannot be fully predictive of the geometry of a system with highly packed molecules such as those studied in the present paper.

Here, we chose to study the structural properties of the system at different levels of formalism: For the monolayers, at different organizations and coverages, the optimized geometrical configuration was obtained through molecular mechanics using the well established polymer-consistent force field (PCFF),[30] which includes nonbonding interactions. For the structural optimization of the isolated molecule absorbed on the clean Si(100) surface, we used both molecular mechanics and *ab initio* DFT calculations, and compared results, hereby establishing the reliability of the methodology. The electronic structure of all systems was addressed by performing full *ab initio* DFT calculations.

We performed state-of-the-art DFT calculations,[31] using the PW91 generalized gradient approximation for the exchange-correlation functional,[32] and *ab initio* ultrasoft pseudopotentials.[33] The single-particle electronic wave functions were expanded in plane waves with a kinetic energy cutoff of 20 Ry. The Si(100) surfaces were modeled by means of repeated slab supercells containing six atomic layers and $\sim$16 Å of vacuum (see Fig. 1). We simulated the (2×1) reconstruction of Si(100) in cells with different lateral periodicity, depending on the coverage: a large $c(16\times16)$ cell was used in the case of single molecule adsorption to isolate a molecule in neighbor cells; and the $p(2\times2)$ cell was used in the case of monolayer configurations. Styrene was adsorbed onto one surface of the slab, while a monolayer of H atoms was used to saturate the dangling bonds on the back side (Fig. 1).

Following the clear evidence reported in Refs. 26 and 27, we assumed, for the adsorption of a single styrene molecule on the Si(100) surface, bonding through cyclo-addition-like reaction leading to a four-atom ring (see Fig. 1 and Sec. III). Using total-energy and force minimization approaches, the clean surface and the single molecule/Si interface were fully relaxed, at the full *ab initio* DFT level, until forces on all atoms were lower than 0.03 eV/Å. In this case, the nonbonding lateral interactions are negligible and the DFT approach can provide an accurate description of the total energy, electronic structure, and geometry of the surface-molecule interface. As said above, we simulated the same system through the PCFF molecular mechanics formalism, also relaxing all atoms. Locally, at the bonding sites, the structural parameters turn out to be very similar. In particular, the DFT results point to local suppression of the dimer-buckling on absorption of the molecule.[34] The maximum difference in bond lengths amounts to 3.5% for the (former) vinylene carbon atoms, and is less than 2% for the other bonds. The tilt angles are also very similar (within 2.6%).

Starting from the same four-atom ring bonding geometry, we considered the sub- and full-monolayer configurations: using PCFF simulations, we obtained the feasible arrangements, and then, keeping fixed the atoms at the PCFF resulting positions, we calculated the corresponding electronic structure at the DFT level. These geometries clearly do not correspond to the ground state of a total energy DFT minimization, however, assuming the overall correctness of the PCFF geometries, the corresponding electronic structures are well characterized by the DFT calculations. The identification of the relative stability of different geometrical configurations, as well as the reaction paths for the chemisorption processes, go beyond the scope of the present manuscript: we focused instead on the understanding of the rationale that correlates the substrate reconstruction and the dosage with the modifications of the band properties of the interface.

III. RESULTS AND DISCUSSION

Our simulation of the clean surface reproduces well the existing experimental[35] and theoretical[36] results: the outermost atoms assemble in buckled dimers along the [011] direction (Fig. 1). The dimerization process can be understood in terms of the formation of a full σ and a weak π double bond. The Si=Si tilting imparts a polar character to the dimer, associated to charge transfer from the "down" to the "up" atom. Accordingly, the lowest unoccupied molecular orbital (LUMO) and the highest occupied molecular orbital (HOMO) are surface states, localized around the "down" and the "up" atom, respectively.

The study of single molecule adsorption provides a great deal of insight into the mechanisms that rule the bonding

properties at the interface. Experimental STM images[13,26] show that styrene is preferentially located along Si dimer rows, and the analysis of infrared adsorption[26] and thermal desorption[27] spectra suggests that the chemisorption of styrene primarily involves the vinyl group. On the basis of the experimental evidence, the starting configuration for the *ab initio* relaxation was obtained by orienting the vinyl group of styrene in proximity to a Si═Si dimer (marked in dark red in Fig. 1). The adsorbed styrene results bridge-bonded to the Si dimer, with the vinyl group only slightly misaligned with respect to the dimer below. The surface does not exhibit structural distortions, except for the adsorption site, where the substrate strongly derelaxes, removing the buckling only of the dimer involved in the bonding process [Fig. 1(b)]. The final product is formally equivalent to a [2+2] cycloaddition reaction,[37] in which the π orbitals of both the alkene C═C and the Si═Si dimer couple and create two covalent Si—C σ bonds in a four-membered Si—Si—C—C ring [Fig. 1(c)]. According to the Woodward-Hoffman selection rules,[3,37] [2+2] cycloaddition reactions between truly double-bonded members (e.g., alkenes) should be symmetry-forbidden. However, the solid-state effects, responsible for the dimer buckling, break the orbital symmetry of the Si double bond, allowing the reaction to occur. The formation of Si—C bonds implies a uniform charge redistribution, which removes the tilting relaxation of the clean dimer [Fig. 1(b)]. Since the binding mechanism involves the vinyl group and a single dimer, the counter-relaxation occurs locally at the adsorption site only, leaving the rest of the surface as well as the phenyl group almost unperturbed.

The electronic structure of the styrene/Si(100) interface confirms the high selectivity of the adsorption process. In Fig. 2(a), we compare the total density of states (DOS) of the Si(100)-2×1 surface with (thin black line) and without (dotted orange line) the presence of the single styrene molecule. The projection on the molecular states (red area) primarily affects the low-energy range of the spectrum, adding new peaks to the original Si-DOS (not shown). The region near the Fermi energy is dominated by the Si states: the HOMO and the LUMO peaks maintain the features of the corresponding states in the clean surface, i.e., localized on the "up" (HOMO) and "down" (LUMO) atoms, respectively. The unique exception is the bonding dimer, where a node of the HOMO and LUMO wave functions is observed [Fig. 2(b)]. To find out the electronic states involving the adsorption site, we have to move away from the Fermi energy toward the continuum of states of the Si surface. The thick black line in Fig. 2(a) represents the DOS projection onto the C atoms of the former vinyl group of styrene and the underlying Si dimer. The peaks closest to the Fermi level are located at −1.0 eV (labeled [2+2] in Fig. 2) and +1.8 eV (labeled [2+2]*), and correspond to the bonding and antibonding states resulting from the cycloaddition reaction, as shown in Fig. 2(b). The formation of the Si—C bonds—energetically more stable than the Si═Si double bond—is responsible for the downward shift of the [2+2] peak. Since the reaction involves only a single dimer (1 out of 16 in our simulation), the adsorption of a single molecule does not significantly modify the electronic properties of the surface around the Fermi energy.

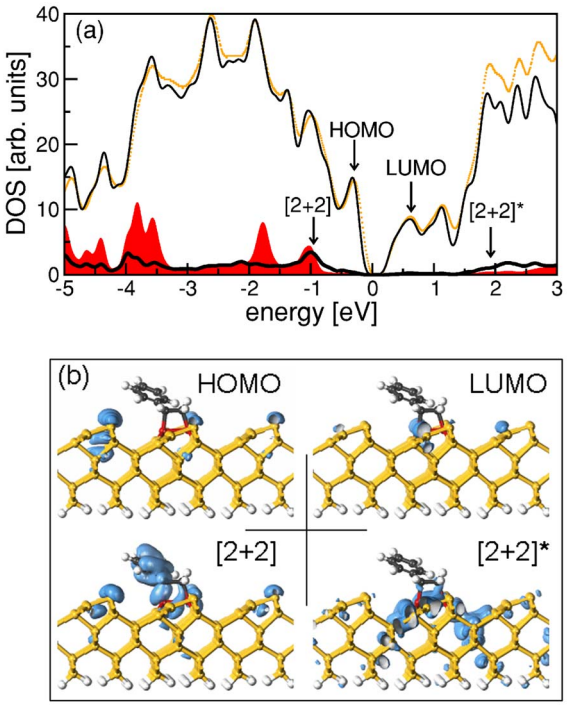

FIG. 2. (Color online) Single molecule adsorption: (a) Total DOS (thin black) and projection on styrene atoms (shaded red area) from styrene/Si(100)-(2×1) interface. Dotted orange line is the total DOS of the clean surface, thick black line is the projection on atoms involved in cycloaddition reaction. Total DOS for clean and adsorbed surfaces are scaled by a factor 0.45 in order to highlight the component projections (shaded red area and thick black line). (b) Isosurface plots of selected single-particle charge densities (side view).

The electronic structure at the edge of the valence band is strongly represented in the simulated STM image [Fig. 3(a)], which was obtained within the Tersoff-Hamman approximation[38] at −2.0 eV bias. We distinguish the uniform pattern of spots related to the upper part of the Si dimers and the bright protrusion centered on the styrene and on the dimer beneath. It is worth noting that the phenyl group, which does not participate in the adsorption process, maintains its original aromatic character.

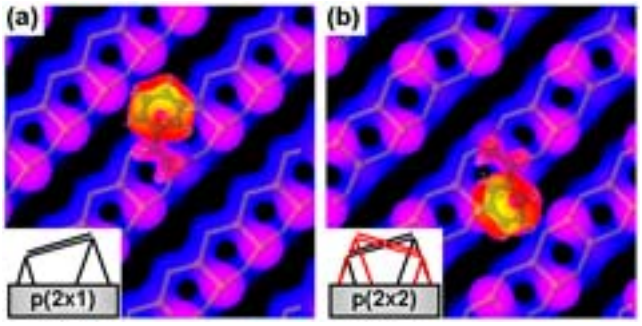

FIG. 3. (Color online) Calculated STM images for single styrene adsorption on Si(100) (a) (2×1) and (b) (2×2) surfaces. Atomic positions of the styrene molecule and of the two outermost Si layers are superimposed for clarity. Insets schematize the different dimer arrangements in the two surface reconstructions.

The simulated STM image agrees well with the experimental results.[13,26] However, at low dosage conditions it has been observed[26] that molecules do not always have the same orientation with respect to the dimer rows, the phenyl group being found on both the right and left sides of a row. To understand this finding, we considered an alternative reconstruction of the Si(100) surface. It is known that Si(100) may undergo different reconstructions depending on the experimental conditions;[35] here we simulated the Si(100)-(2×2) surface, which is characterized by parallel rows of alternating buckled dimers along the [011] direction. Results for the adsorption of a single styrene onto this surface are displayed in Fig. 3(b). The alternating spots in the STM image reflect the alternating orientation of the Si=Si dimers, and no significant changes are observed close to the bonded molecule. The adsorption mechanism is the same as for the (2×1) case: since the [2+2] cycloaddition involves a single Si=Si site, the relative orientation of the dimers does not modify the bonding properties at the interface, driving only the lateral orientation of the phenyl group.

Increasing the dosage, styrene adsorbs on Si(100) at a saturation coverage of 1 monolayer (ML), which corresponds to one styrene for every surface dimer.[27] The self-assembled overlayer is highly ordered and oriented along the dimer rows, with an intermolecular distance of 3.8 Å along the [011] direction, induced by the substrate periodicity. Here, we considered the adsorption of styrene molecules at 1 ML coverage, on both the Si(100)-(2×1) and the -(2×2) surfaces [Figs. 4(a) and 4(b)]. We labeled the former system [1 ML@(2×1)] and the latter [1 ML@(2×2)], where the internal parentheses refer to the original substrate reconstruction.

In the two cases, the molecule/surface bonding is referable to a [2+2] cycloaddition reaction, through the formation of a four-membered ring for each adsorbed molecule. However, at full monolayer the different Si(100) reconstructions may result in different steric couplings among the molecules. The outermost characteristics of the surface impart a specific order to the overlayer, acting as a programmable template for the growth of the organic material. Thus the monotonic buckling of (2×1) reconstruction leads to a parallel arrangement of the phenyl groups, which align vertically along one side of the dimer row [Fig. 4(a)]. The (2×2) reconstruction causes, instead, a zigzag alternation of the aromatic rings, which arrange in a herringbone structure along the [011] direction [Fig. 4(b)].

Despite the different spatial arrangement of the overlayers, the two systems present interesting similarities in their electronic structures: the analysis of the interface reveals two major effects, related to Si dimer-vinyl and to phenyl-phenyl interactions, respectively. The former concerns the bonding properties at the Si/molecule interface. Since the styrene chemisorption is site-specific and highly localized, the monolayer configuration turns out to be a simple superposition of single adsorption events. Following the lines described above, for each bonded molecule we observe the breaking of Si-dimer double bonds and the formation of bonding [labeled [2+2] in Fig. 5(b)] and antibonding Si—C orbitals, lying in the region of continuum bulk states of the surface (see Fig. 6). In the limit of full coverage, where all dimers are saturated, we notice the complete suppression of the original HOMO and LUMO peaks of the clean surface, which were representative of the Si=Si double bonds. The HOMO and LUMO peaks of the fully covered surface are the result of the hybridization of Si-bulk and Si—C states, as shown in Figs. 5(b) and 6 for the [1 ML@(2×1)] structure. The overall effect of the overlayer formation is the opening of the band gap.

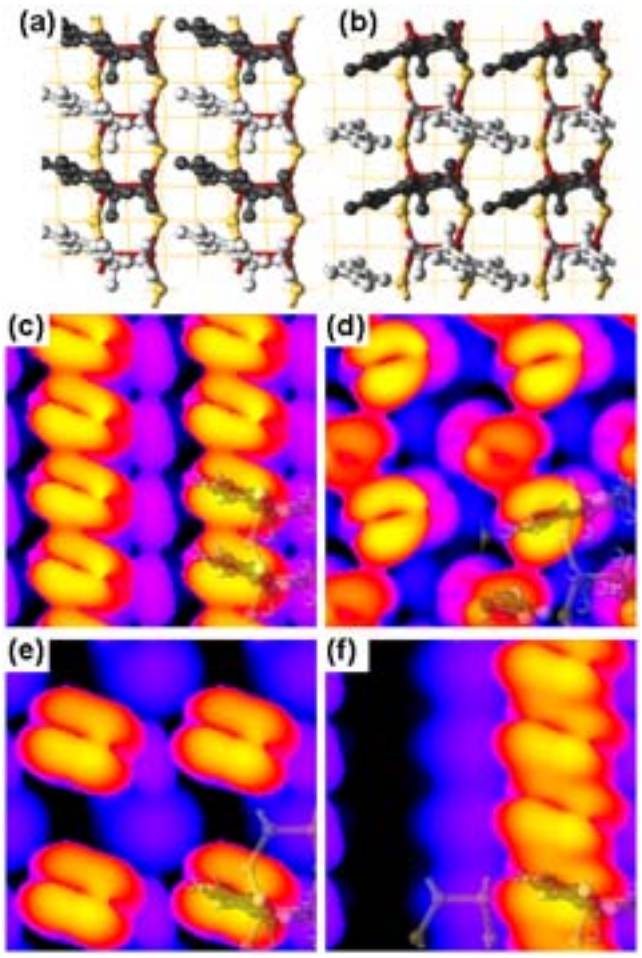

FIG. 4. (Color online) Top panel: optimized atomic geometries for styrene molecules adsorbed on Si(100)-(2×1) (a) and (2×2) (b) reconstructions at 1 ML coverage, namely $[1\ \mathrm{ML@}(2\times1)]_{(2\times2)}$ and $[1\ \mathrm{ML@}(2\times1)]_{(2\times2)}$ configurations, respectively. Ball-stick rendering corresponds to styrene molecules and to the two outermost Si layers, thin lines to planes beneath. Red atoms mark the unbuckled Si dimers. Styrene molecules are alternately colored (light vs dark gray) for clarity. Middle panel: calculated STM images for 1 ML coverage on (2×1) (c) and (2×2) (d) surface reconstructions, corresponding to the structures (a) and (b), respectively. Bottom panel: 0.5 ML coverage configurations on Si(100)-(2×1) substrate with (2×2) (e) and (4×1) (f) lateral periodicity. Atoms of unit cells are superimposed for clarity.

To understand this, we compare (Fig. 5) the DOS of clean -(2×1) (solid line) and -(2×2) (dashed line) reconstructions [panel (a)] with the corresponding functionalized surfaces [panel (b)]. The two curves for the clean surfaces [panel (a)] are quite similar (the slight discrepancies are due

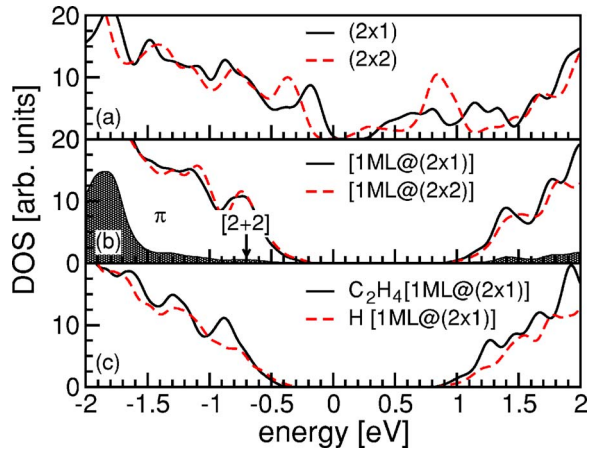

FIG. 5. (Color online) Density of states near the band gaps for (a) clean Si(100)-(2×1) and (2×2) reconstructions; (b) styrene adsorption on (2×1) and (2×2) Si substrate at 1 ML coverage; (c) ethylene (C_2H_4) molecule and H atom adsorption on Si(100)-(2×1) at full monolayer coverage. In panel (b) the shaded area is the projected-DOS on styrene atoms for the [1 ML@(2×1)] configuration. All curves were aligned by the lowest valence-band silicon states. Zero energy reference corresponds to the Fermi level of the (2×1) clean surface.

to the specific relaxation mechanisms): they are both characterized by a small gap caused by the presence of surface states in the original Si gap.[39] In the monolayer configuration [panel (b)], these states completely disappear, opening the band gap. It is worth noting that the DOS's of panel (b) are almost identical, indicating that the band-gap variation depends only on the Si-dimer saturation (i.e., the Si-vinyl interaction) and not on the details of the starting surface reconstruction or of the overlayer arrangement. To support this hypothesis, we studied the case of ethylene (C_2H_4) and monohydride adsorption on the Si(100)-(2×1) surface at 1 ML coverage. Figure 5(c) shows the same gap enlargement as in the styrene case; the further features related to the specific adsorbate (e.g., the vinyl group in ethylene) affect the DOS only in other energy regions. This confirms that the gap opening is ruled only by the saturation process of the exposed dimers, and not by other fragments (e.g., the phenyl group of styrene).

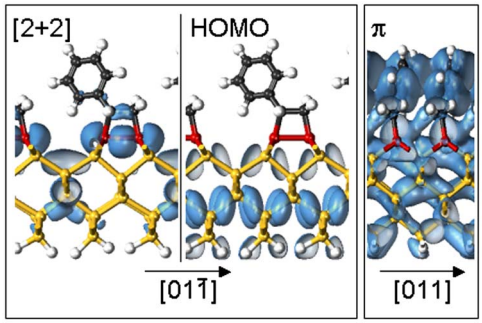

FIG. 6. (Color online) Adsorption of styrene molecules on Si(100)-(2×1) surface ([1 ML@(2×1)] in the text) at full coverage configuration. Isosurface plots of selected single-particle states (side views). Labels refer to Fig. 5(b).

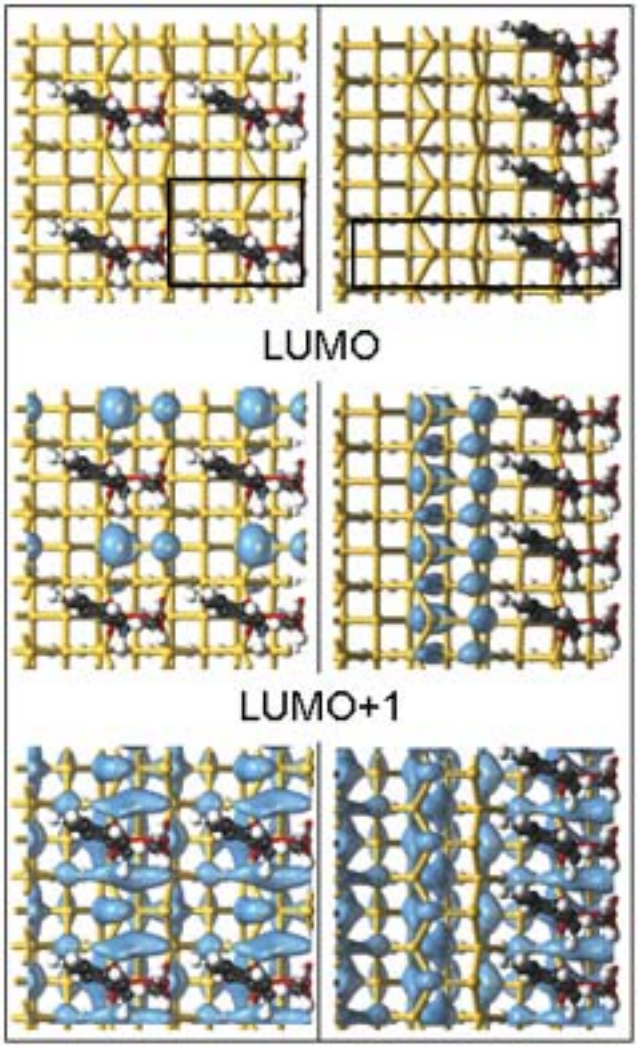

FIG. 7. (Color online) Styrene adsorption on Si(100)-(2×1) surface at 0.5 ML for the $[0.5\ \mathrm{ML}@(2\times1)]_{(2\times2)}$ (left panel) and $[0.5\ \mathrm{ML}@(2\times1)]_{(4\times1)}$ (right panel) configuration. Top view of isosurface plots of LUMO (middle panel) and LUMO+1 (bottom panel). Dark straight lines identify the (2×2) (left) and (4×1) (right) lateral unit cells used in the simulations.

Along these lines, we considered further intermediate configurations, where only a part of the original Si surface states are saturated. Two reconstructions for the styrene adsorbed on Si(100)-(2×1) at 0.5 ML coverage are considered. The first ($[0.5\ \mathrm{ML}@(2\times1)]_{(2\times2)}$) is a (2×2) structure, where each dimer row is constituted of the alternation of buckled dimers and styrene molecules along the [011] direction (see Fig. 7, left panel). The second ($[0.5\ \mathrm{ML}@(2\times1)]_{(4\times1)}$) has a (4×1) periodicity and consists in the alternation along the $[01\bar{1}]$ direction of an unperturbed Si-dimer row and a styrene-saturated row (see Fig. 7, right panel). In both cases, 50% of Si-dimers persist in the clean surface configuration. Here we focused only on the modification of the electronic properties owing to the different arrangement of exposed dimers.[40] The resulting DOS's are shown in Fig. 8. We focused on the modification of the frontier orbitals with respect to the Si-dimer surface states of

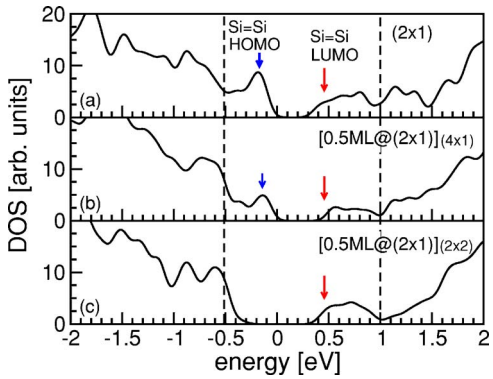

FIG. 8. (Color online) Modification of Si-dimer HOMO (blue arrows) and LUMO (red arrows) peaks of the clean (2×1) surface (a) at 0.5 ML coverage, for the (4×1) (b) and (2×2) (c) reconstructions. Vertical dashed lines correspond to the energy gap at saturation (see Fig. 5). All curves were aligned as in Fig. 5.

the clean substrate [Fig. 8(a)]. The vertical lines indicate the large gap at saturation conditions [Figs. 5(b) and 5(c)].

The $[0.5\ \mathrm{ML@}(2\times1)]_{(4\times1)}$ structure presents common features to both the clean and the fully saturated system: the energy gap is similar to that of the clean surface. The HOMO and LUMO peaks (vertical arrows) correspond to the unperturbed Si-dimers and have a halved intensity. The presence of the styrene introduces spectral features about −1 eV, outside the full saturation gap (vertical lines), as in the 1 ML case. On the contrary, the on-row alternation in the $[0.5\ \mathrm{ML@}(2\times1)]_{(2\times2)}$ system breaks the intrinsic coupling among dimers, suppressing the HOMO peak but leaving states in the region of the LUMO peak of the clean surface. Indeed, the resulting band gap is larger than for the clean surface but smaller than for the fully covered system. It is worth noting that the HOMO peak is more sensitive to the adsorption of the molecule, while the LUMO maintains its original character in the two reconstructions [Figs. 8(b) and 8(c)]. In both cases, the LUMO states are localized around the unsatured dimers (Fig. 7, middle panel) and the LUMO+1 are bulklike silicon states (Fig. 7, bottom panel), delocalized on the whole structure, except the molecule. On the basis of these results, we suggest that the functionalized surfaces at submonolayer coverage—even with less ordered overlayers—may act as a 2D layer of electron acceptors, and promote the charge transport through the silicon conduction states. We conclude that it should be possible to tune the band gap and the conduction properties of the interface by controlling the coverage of the adsorbed molecules.

At 1 ML coverages, a broadening of the π peaks deriving from the aromatic rings [Fig. 5(b)] reveals the presence of a phenyl-phenyl interaction. This is a signature of the π-π interaction between the assembled molecules that tends to create delocalized orbitals at the surface: The closer the packing, the higher is the superposition of the molecular orbitals. The formation of dispersive states (see Fig. 6, right panel) may in principle enhance the in-plane transport properties of the organic overlayer.

The specific relative orientation among the aromatic rings plays a crucial role in the expected efficiency for intermolecular transport. Despite their similar band-structure properties, the 1 ML coverages on the (2×1) and (2×2) reconstructions give rise to cofacial and herringbone arrangements, respectively [Figs. 4(a) and 4(b)], which lead to different in-plane transport efficiencies: the direct π-π organization typically results in electronic transfer integrals that are one order of magnitude larger than in the herringbone structure.[41] Besides the (2×1) reconstruction for the 1 ML coverage, we argue that also the (4×1) reconstructions for the 0.5 ML coverage might originate satisfactory hole transport performances along the styrene-saturated 1D rows.

The different arrangements of the overlayer may be distinguished through the analysis of the delocalized π-channels, by means of STM experiments. In Figs. 4(c)–4(f), we show the calculated STM images for the target systems, in good agreement with the experimental ones.[13,26] The current signal is stronger in the $[1\ \mathrm{ML@}(2\times1)]$ structure, which realizes the maximum π-π superposition. The π-channels expand parallel to the dimer rows, while they are almost localized in the perpendicular direction [Figs. 4(c) and 4(f)]. This implies that the directional Si-dimer motif of the clean surface drives also the formation of an ordered pattern of electronic wires on top of the surface, which may be appealing for further nanoscale applications. It is worth noting that these electronic features, given by the phenyl-phenyl interaction, cannot be obtained with other adsorbates such as hydrogen or ethylene.

IV. CONCLUSIONS

In conclusion, we studied the effects of styrene adsorption on two reconstructed Si(100) surfaces, at different coverage configurations. We focused on the electronic structure of the system, highlighting the effects of the Si—C bond formation on the overall properties at different submonolayer coverage configurations. The localized and directional nature of the Si-dimer rows governs both the atomic structure and the conduction properties of the overlayer. Our results show different regimes as a function of substrate reconstruction and of the dosage separately: the former is responsible for the final arrangement of the molecular monolayer (e.g., cofacial versus herringbone); the latter drives the conduction properties and the electron distribution of the interface. While at high coverage (e.g., $[1\ \mathrm{ML@}(2\times1)]$) the effective π-π coupling may induce hole transport through the molecular layer, it is interesting to note that at submonolayer regimes electron transport along the surface-layer Si states is favored.

ACKNOWLEDGMENTS

This work was supported by MIUR (Italy) through grant FIRB-Nomade and by INFM-CNR through "Progetto calcolo parallelo." We thank C.S. Cucinotta and R. Di Felice for fruitful discussions.

*Author to whom all correspondence should be addressed. Email address: calzolari.arrigo@unimore.it

[1] J. T. Yates, Jr., Science **279**, 335 (1998).
[2] M. C. Hersam, N. P. Guisinger, and J. W. Lyding, Nanotechnology **11**, 70 (2000).
[3] S. F. Bent, Surf. Sci. **500**, 879 (2002).
[4] F. Schreiber, Prog. Surf. Sci. **65**, 151 (2000).
[5] G. P. Lopinski, D. D. M. Wayner, and R. A. Wolkow, Nature (London) **406**, 48 (2000).
[6] C. R. Kinser, M. J. Schmitz, and M. C. Hersam, Nano Lett. **5**, 91 (2005).
[7] R. Basu, N. P. Guisinger, M. E. Greene, and M. C. Hersam, Appl. Phys. Lett. **85**, 2619 (2004).
[8] H. Liu and R. J. Hamers, J. Am. Chem. Soc. **119**, 7593 (1997).
[9] S. H. Xu *et al.*, Phys. Rev. Lett. **84**, 939 (2000).
[10] S. K. Coulter, J. S. Hovis, M. D. Ellison, and R. J. Hamers, J. Vac. Sci. Technol. A **18**, 1965 (2000).
[11] R. J. Hamers, J. S. Hovis, S. Lee, H. Liu, and J. Shan, J. Phys. Chem. B **101**, 1489 (1997).
[12] N. P. Guisinger, N. L. Yoder, and M. C. Hersam, Proc. Natl. Acad. Sci. U.S.A. **102**, 8838 (2005).
[13] N. P. Guisinger, M. E. Green, R. Basu, A. S. Baluch, and M. C. Hersam, Nano Lett. **4**, 55 (2004).
[14] N. P. Guisinger, M. E. Green, R. Basu, A. S. Baluch, and M. C. Hersam, Nanotechnology **15**, S452 (2004).
[15] T. Rakshit, G.-C. Liang, A. W. Ghosh, and S. Datta, Nano Lett. **4**, 1803 (2004).
[16] J. K. Kang and C. B. Musgrave, J. Chem. Phys. **116**, 9907 (2002).
[17] J. H. Cho, D. H. Oh, and L. Kleinman, Phys. Rev. B **65**, 081310(R) (2002).
[18] A. Rochefort and A. Beausoleil, Chem. Phys. Lett. **400**, 347 (2004).
[19] N. Takeuchi, Y. Kanai, and A. Selloni, J. Am. Chem. Soc. **126**, 15890 (2004).
[20] N. Takeuchi and A. Selloni, J. Phys. Chem. B **109**, 11967 (2005).
[21] Y. Kanai *et al.*, J. Phys. Chem. B **109**, 13656 (2005).
[22] K. Seino, W. G. Schmidt, and F. Bechstedt, Phys. Rev. B **69**, 245309 (2004).
[23] C. Cucinotta, A. Ruini, E. Molinari, and M. J. Caldas, J. Phys. Chem. B **108**, 17278 (2004).
[24] A. C. Ferraz and R. Miotto, Surf. Sci. **566**, 713 (2004).
[25] Y. Wang, J. Ma, S. Inagaki, and Y. Pei, J. Phys. Chem. B **109**, 5199 (2005).
[26] M. P. Schwartz, M. D. Ellison, S. K. Coulter, J. S. Hovis, and R. J. Hamers, J. Am. Chem. Soc. **122**, 8529 (2000).
[27] Q. Li and K. T. Leung, J. Phys. Chem. B **109**, 1420 (2005).
[28] N. A. Lima and M. J. Caldas, Phys. Rev. B **72**, 033109 (2005).
[29] M. Alves-Santos *et al.*, J. Comput. Chem. **27**, 217 (2006).
[30] M. J. Hwang, T. P. Stockfisch, and A. T. Hagler, J. Am. Chem. Soc. **116**, 2515 (1994).
[31] Computer code: PWSCF by S. Baroni *et al.* (www.pwscf.org.).
[32] J. P. Perdew and Y. Wang, Phys. Rev. B **33**, R8800 (1986).
[33] D. Vanderbilt, Phys. Rev. B **41**, 7892 (1990).
[34] The description of the clean surface is less accurate with the molecular mechanics formalism since, while it includes nonbonded interactions that are of interest when describing the intermolecular arrangement, it does not include the electronic structure effects and thus cannot describe the dimer buckling characteristic of this particular surface.
[35] C. B. Duke, Chem. Rev. (Washington, D.C.) **96**, 1237 (1996).
[36] A. Ramstad, G. Brocks, and P. J. Kelly, Phys. Rev. B **51**, 14504 (1995).
[37] R. J. Hamers, S. K. Coulter, M. D. Ellison, J. S. Hovis, D. F. Padowitz, M. P. Schwartz, C. M. Greenlief, and J. N. Russel, Acc. Chem. Res. **33**, 617 (2000).
[38] J. Tersoff and D. R. Hamann, Phys. Rev. B **31**, 805 (1985).
[39] We are aware of the problems related to the band-gap evaluation in DFT supercell calculations, namely two antithetic effects: the underestimation of the DFT band gap, and the gap opening due to the finite size of the surface slab. Here, we are interested in the mechanisms that rule the gap control at interface, while its exact evaluation goes beyond the aim of this work.
[40] The identification of the true stable submonolayer phase goes beyond the aim of this work: Even though the 2×2 configuration results energetically more stable than the 4×1 configuration, a direct comparison of the total energies is not significant, because of the lack of the nonbonding interactions in DFT calculations.
[41] A. Ferretti, A. Ruini, E. Molinari, and M. J. Caldas, Phys. Rev. Lett. **90**, 086401 (2003).